




Comparison of ^{64}Cu -DOTA-PSMA-3Q and ^{64}Cu -NOTA-PSMA-3Q utilizing NOTA and DOTA as bifunctional chelators in prostate cancer: preclinical assessment and preliminary clinical PET/CT imaging

Huanhuan Liu^{1,2} · Xiaojun Zhang¹ · Jingfeng Zhang^{1,2} · Yue Pan^{1,2} · Hui Wen¹ · Xiaodan Xu¹ · Shina Wu¹ · Yuan Wang¹ · Cong Zhang^{1,2} · Guangyu Ma¹ · Yachao Liu¹ · Ruimin Wang¹ · Jinming Zhang¹ 

Received: 20 December 2024 / Accepted: 3 February 2025 / Published online: 15 February 2025

© The Author(s) 2025

Abstract

Objective This study aims to investigate the efficacy and safety of prostate-specific membrane antigen (PSMA) radiolabeled with copper-64 (^{64}Cu) using the bifunctional chelating agents (BFCAs) NOTA (1,4,7-triazacyclononane-1,4,7-triacetic acid) and DOTA (1,4,7,10-tetraazacyclododecane-1,4,7,10-tetraacetic acid). As widely utilized BFCAs in the development of radiopharmaceuticals, NOTA and DOTA play a critical role in ensuring stable chelation with ^{64}Cu . This study evaluates the stability, bioavailability, and therapeutic potential of these radiolabeled compounds in preclinical models and initial clinical trials.

Methods ^{64}Cu -DOTA-PSMA-3Q and ^{64}Cu -NOTA-PSMA-3Q were synthesized by manual labeling. The radiochemical purity, stability, specificity and biological distribution of the product were evaluated by preclinical studies. In 23 patients with suspected prostate cancer, PET/CT imaging was used to evaluate the potential and differences in biological distribution of ^{64}Cu -DOTA-PSMA-3Q and ^{64}Cu -NOTA-PSMA-3Q in clinical diagnosis.

Results The radiochemical purities of ^{64}Cu -DOTA-PSMA-3Q and ^{64}Cu -NOTA-PSMA-3Q are more than 98% and have good stability in vitro. Biodistribution studies in healthy mice revealed that both tracers primarily underwent renal excretion post-injection. Liver uptake of ^{64}Cu -DOTA-PSMA-3Q was significantly higher than that of ^{64}Cu -NOTA-PSMA-3Q at 1 h after injection ($P < 0.05$). Micro-PET/CT imaging in 22Rv1 tumor-bearing mice demonstrated similar tumor uptake for both tracers at 1 h after injection ($P > 0.05$). However, after 24 h, ^{64}Cu -DOTA-PSMA-3Q exhibited significantly better tumor retention compared to ^{64}Cu -NOTA-PSMA-3Q ($P < 0.05$). In clinical PET/CT imaging involving 23 patients with suspected prostate cancer, no adverse reactions or significant changes in vital signs were observed, underscoring the safety of both tracers. Notably, ^{64}Cu -NOTA-PSMA-3Q demonstrated higher uptake in the lacrimal glands (17.73 vs. 10.84), parotid glands (20.98 vs. 16.30), and submandibular glands (20.26 vs. 17.28) compared to ^{64}Cu -DOTA-PSMA-3Q. Conversely, uptake in the sublingual glands was lower for ^{64}Cu -NOTA-PSMA-3Q (7.10 vs. 7.49). Of particular clinical relevance, liver uptake of ^{64}Cu -NOTA-PSMA-3Q was significantly lower than that of ^{64}Cu -DOTA-PSMA-3Q (4.04 vs. 8.18), highlighting a key difference in their biodistribution profiles.

Conclusions Both NOTA and DOTA are suitable chelators for the development of ^{64}Cu -labeled PSMA-3Q tracers for PET/CT imaging. DOTA showed better tumor retention 24 h after injection, while NOTA showed lower uptake in the liver, in addition, NOTA was higher uptake in the salivary glands, while DOTA was lower uptake in these tissues. Overall, these findings highlight the importance of selecting the right chelating agent to optimize clinical imaging outcomes.

Trial registration Chinese Clinical Trial Registry ChiCTR2300072655, Registered 20 June 2023.

Keywords ^{64}Cu -NOTA-PSMA-3Q · ^{64}Cu -DOTA-PSMA-3 · QPSMA-PET/CT · Prostate cancer · Bifunctional chelating agent

Huanhuan Liu, Xiaojun Zhang and Jingfeng Zhang contributed equally to this work.

Extended author information available on the last page of the article

Introduction

Prostate cancer (PCa) ranks as one of the most common malignancies among men globally and is the second leading cause of cancer-related death among men worldwide. It continues to pose a significant health burden, with an estimated 1.4 million new cases and around 400,000 deaths annually. These high incidence and mortality rates are largely driven by advancements in diagnostic and therapeutic technologies. The management landscape of PCa is undergoing rapid evolution, with imaging playing a crucial role in early diagnosis, treatment planning, treatment response monitoring, and follow-up of patients [1, 2]. Prostate-specific membrane antigen (PSMA) positron emission tomography (PET)/computed tomography (CT) is increasingly becoming the preferred imaging modality for PCa worldwide, offering improved staging accuracy across nearly all disease stages. PSMA-PET imaging is progressively supplanting traditional imaging methods [3, 4]. Furthermore, the inclusion of PSMA-PET in clinical guidelines and consensus documents as a first-line option for the staging and restaging of primary prostate cancer underscores its growing importance in the personalized management of PCa [5]. However, the enhanced sensitivity of this imaging modality presents new challenges in clinical management. Although PSMA PET imaging has been recognized in clinical guidelines and consensus documents for its superior diagnostic accuracy compared to conventional imaging, it remains uncertain whether this enhanced sensitivity and earlier detection will translate into significant improvements in patient outcomes [6].

In addition to advances in imaging, the therapeutic landscape for PCa is being reshaped by the development of PSMA-targeted drugs and radiotracers. Several promising agents, including ^{18}F -DCFPyL, ^{68}Ga -PSMA-11, ^{68}Ga -PSMA-617, ^{18}F -PSMA-1007, and ^{68}Ga -PSMA-I&T, have either received FDA approval or are currently undergoing clinical evaluation [7]. While these agents have significantly improved the detection of primary tumors and metastases, radiotracers capable of extending the imaging window are still needed to accommodate growing clinical needs. This is where the radioactive labeling of PSMA tracers with the positron-emitting isotope ^{64}Cu presents a compelling advantage [8]. ^{64}Cu is a positron emitter with a half-life of 12.7 h, significantly longer than that of commonly used imaging isotopes like ^{18}F ($T_{1/2} = 109$ min) and ^{68}Ga ($T_{1/2} = 68$ minutes). This extended half-life allows for more flexible scheduling of PET scans and the possibility of imaging sites far from cyclotron facilities, thereby improving access to advanced imaging technology. Furthermore, ^{64}Cu has a versatile decay profile that includes 18% positron (β^+) and 39% beta (β^-) emissions, making it suitable for both diagnostic PET imaging and radionuclide therapy. Its decay via

electron capture also results in the emission of Auger electrons, which contribute to cytotoxic effects at the cellular level [9]. This unique combination of decay mechanisms provides an opportunity for ^{64}Cu to function as a theranostic agent, offering both diagnostic and therapeutic applications. Notably, ^{64}Cu can be paired with its therapeutic counterpart, ^{67}Cu , to form a theranostic pair, enabling integrated imaging and targeted radiotherapy for prostate cancer [10].

1,4,7,10-Tetraazacyclododecane-1,4,7,10-tetraacetic acid (DOTA) is one of the most extensively studied bifunctional chelators (BFCs) for radiolabeling with ^{64}Cu . Despite its widespread use, several studies have highlighted the relatively low thermodynamic and kinetic stability of ^{64}Cu -DOTA complexes in vivo. This instability can result in demetallation, leading to off-target accumulation of ^{64}Cu in non-target tissues, particularly the liver [11–15]. Such accumulation poses a challenge for clinical applications where high tracer specificity and minimal background signal are essential. Recent comparative studies have provided valuable insights into the performance differences between DOTA and 1,4,7-triazacyclononane-1,4,7-triacetic acid (NOTA) as chelators for ^{64}Cu in prostate cancer imaging. Lee, Inki, et al. reported that ^{64}Cu -labeled DOTA (^{64}Cu -cudotadipep) exhibited higher uptake in target tissues than its NOTA-labeled counterpart (^{64}Cu -cunotadipep). However, this benefit was offset by a significant increase in liver uptake for the DOTA chelator. Conversely, the NOTA chelator demonstrated higher in vivo kinetic stability, resulting in minimal dissociation of ^{64}Cu and reduced hepatic accumulation [11]. These findings underscore the significant role that chelator structure plays in determining the in vivo stability and biodistribution of radiopharmaceuticals, highlighting the importance of chelator selection during radio-tracer development [16].

Building on these insights, we recently conducted a clinical study utilizing ^{64}Cu -DOTA-PSMA-3Q to facilitate real-time diagnosis during image-guided biopsies of prostate cancer [17]. This radiation-guided approach offers a significant advancement in PSMA-PET image-guided biopsy procedures, enabling real-time verification of lesion sampling during the biopsy process. By providing immediate confirmation of sample accuracy, this technique enhances the reliability of biopsy results, reduces the likelihood of missed targets, and ultimately optimizes clinical outcomes. Our initial findings demonstrated the diagnostic efficacy of ^{64}Cu -DOTA-PSMA-3Q; however, liver uptake associated with the in vivo instability of the ^{64}Cu -DOTA complex remains a concern. Although this limitation did not compromise diagnostic performance, it underscores the need for improvements in chelator selection to enhance imaging specificity and reduce off-target uptake.

To address this challenge, we propose the use of NOTA as an alternative chelating agent for labeling PSMA-3Q with ^{64}Cu . Given the superior kinetic stability and reduced dissociation of ^{64}Cu observed with NOTA in previous studies, we hypothesize that NOTA-labeled ^{64}Cu -PSMA-3Q will exhibit lower liver uptake and improved biodistribution compared to its DOTA-labeled counterpart. These potential enhancements could have significant clinical implications for prostate cancer imaging, particularly in reducing off-target signal and improving tumor-to-background ratios in PET/CT imaging.

This study focuses on the development and evaluation of ^{64}Cu -labeled PSMA tracers using the bifunctional chelating agents (BFCAs) NOTA (1,4,7-triazacyclononane-1,4,7-triacetic acid) and DOTA (1,4,7,10-tetraazacyclododecane-1,4,7,10-tetraacetic acid). These chelators play a critical role in ensuring strong and stable chelation of ^{64}Cu , a prerequisite for effective PET imaging and therapy. By leveraging the unique properties of NOTA and DOTA, this study aims to assess the stability, biodistribution, imaging efficacy, and safety of ^{64}Cu -DOTA-PSMA-3Q and ^{64}Cu -NOTA-PSMA-3Q in both preclinical and clinical settings. The ultimate goal is to identify the optimal chelator for ^{64}Cu -based PSMA tracers, thereby enhancing the clinical utility of PSMA-PET imaging for prostate cancer management.

Materials and methods

All chemicals, solvents, and reagents used were of analytical grade and procured from McLink Biochemical Technology Co., Ltd. (Shanghai, China). The ^{64}Cu radionuclide was supplied by Guangdong Huashuo Molecular Imaging Technology Co., Ltd. (Guangdong, China). Radioactivity measurements were conducted using a CRC-25R dose calibrator (Capintec, INC, USA) and a γ -Counter (AMG 425–601, Hidex, Finland). The radiochemical purity were assessed using a high-performance liquid chromatography (HPLC, Waters, USA). Small-animal PET scans were performed with a Super Nova PET/CT scanner (Ping sheng Medical Technology Co., Ltd.). BALB/c nude mice, aged 3–4 weeks and weighing 13–15 g, were procured from Charles River Laboratory (Beijing, China). About 5×10^6 cells were implanted into the right shoulder of each mouse. Imaging experiments were conducted on tumor-bearing mice once the tumor volume reached 200–300 mm³. All procedures involving animals were performed in compliance with the protocols approved by the Animal Protection and Utilization Committee of the First Medical Center of the Chinese People's Liberation Army General Hospital (approval number: S2023-295-01). The experimental animals were kept in a temperature of $22 \pm 2^\circ\text{C}$, humidity of 50–70%, 12-hour

light and dark cycle, good ventilation and hygiene management to ensure the health of animals and the reliability of experimental results.

^{64}Cu -labelled NOTA-PSMA-3Q and DOTA-PSMA-3Q, quality control, in vitro stability and partition coefficient

Detailed information on reagents, chemicals, high-performance liquid chromatography (HPLC), liquid chromatography-mass spectrometry (LC-MS), and synthesis flowcharts for NOTA-PSMA-3Q and DOTA-PSMA-3Q is available in the supplementary materials previously published by our research group [17, 18]. Detailed information on radioactive synthesis and quality control procedures is provided in the supplementary material.

Radiotoxicity of ^{64}Cu -NOTA-PSMA-3Q, biodistribution and micro-PET imaging

Healthy BALB/c male mice were administered either ^{64}Cu -NOTA-PSMA-3Q (37 MBq, 150 μL) or normal saline (150 μL) to assess radiotoxicity.

In biodistribution experiments, These mice were randomly divided into four groups ($n=3$ per group) and received injections of ^{64}Cu -DOTA-PSMA-3Q or ^{64}Cu -NOTA-PSMA-3Q (1.48 MBq, 100 μL). Mice were sacrificed at 1, 4, 12, and 24 h post-injection (p.i.). Tissues and organs of interest were collected, weighed, and their radioactivity was measured using a gamma counter. The radioactive uptake rate (%ID/g) for each tissue and organ was calculated after radioactivity decay correction.

In Micro-PET imaging experiments, groups of 22RV1 tumor xenograft models ($n=3$) were injected via the tail vein with ^{64}Cu -DOTA-PSMA-3Q or ^{64}Cu -NOTA-PSMA-3Q (ranging from 5.55 to 7.4 MBq, 150 μL per mouse). Ten-minute static PET scans were conducted at 1, 4, 12, and 24 h after injection. ZJ-43 ((S)-2-(3-((S)-1-carboxy-3-methylbutyl)ureido), pentanedioic acid) was utilized as a blocking agent for PSMA (Fig. S3). (for all of the details see the supplementary materials).

Preliminary clinical PET/CT imaging in humans

Preliminary clinical research was approved by the Ethics Committee of the First Medical Center of the Chinese People's Liberation Army General Hospital (approval number: S2023-208-02) and registered at the Chinese Clinical Trial Registry (ChiCTR2300072655). The study recruited 23 patients with suspected prostate cancer who provided informed consent. Patients were divided into two groups: 11 patients underwent PET/CT scans with

^{64}Cu -NOTA-PSMA-3Q, and 12 patients underwent scans with ^{64}Cu -DOTA-PSMA-3Q, as outlined in Table 1. Each patient received an intravenous injection of 148 MBq of the respective tracer, followed by PET/CT imaging 2 h post-injection. The scans, covering the region from the base of the skull to the upper thigh, were performed using a uEXPLORER scanner (United Imaging Healthcare, China). Image reconstruction utilized the ordered subsets expectation maximization (OSEM) algorithm with time-of-flight (TOF) and point spread function (PSF) corrections. Reconstruction settings included 3 iterations, 20 subsets, a 256×256 matrix, a 600 mm field of view, a 1.443 mm slice thickness, Gaussian post-filtering, and a 2 mm full width at half maximum (FWHM). PET/CT images were independently analyzed by two experienced physicians, who measured the maximum standardized uptake value (SUVmax) for each lesion as well as for normal organs, ensuring reliable and unbiased evaluation of tracer uptake.

Statistical analysis

Statistical analyses were conducted using SPSS version 26.0 (New York, USA, May 2019) and GraphPad Prism version 8.0 (San Diego, USA). A p -value < 0.05 was considered indicative of statistical significance. Data that conformed to a normal distribution were reported as mean \pm standard deviation (SD), while non-normally distributed data were presented as median and interquartile ranges (IQR) to accurately capture dispersion. For comparisons involving normally distributed data, independent sample t -tests and tests for homogeneity of variance were applied. In cases where the data did not follow a normal distribution, the Wilcoxon rank sum test was used as a non-parametric alternative to assess differences between groups. This comprehensive statistical approach ensured appropriate analysis of the

data, accounting for both parametric and non-parametric distributions.

Results

Radiolabeling, quality control and characterization of the ^{64}Cu -labelled NOTA-PSMA-3Q and DOTA-PSMA-3Q

The radiochemical purity of ^{64}Cu -NOTA-PSMA-3Q and ^{64}Cu -DOTA-PSMA-3Q was more than 98%. The log P values for ^{64}Cu -NOTA-PSMA-3Q and ^{64}Cu -DOTA-PSMA-3Q were determined to be -2.61 ± 0.03 and -2.34 ± 0.08 , respectively, indicating that ^{64}Cu -NOTA-PSMA-3Q exhibits greater hydrophilicity compared to ^{64}Cu -DOTA-PSMA-3Q. High performance liquid chromatography (HPLC) analysis showed that ^{64}Cu -NOTA-PSMA-3Q showed good stability during the test (Fig. S2). Additional information on the quality control procedures can be found in the Supplementary Materials (Fig. S1). The stability of ^{64}Cu -DOTA-PSMA-3Q has been demonstrated in previous studies.

Radiotoxicity of ^{64}Cu -NOTA-PSMA-3Q, biodistribution and Micro-PET imaging

Mice injected with ^{64}Cu -NOTA-PSMA-3Q or normal saline exhibited no mortality within 14 days, with no significant differences observed between the two groups in terms of body weight, diet, excretion, activity level, mental status, or skin condition throughout the observation period. Histological analysis of major organs, visualized using H&E staining, showed no detectable pathological changes or differences between the two groups (Fig. S2), supporting the safety of ^{64}Cu -NOTA-PSMA-3Q in vivo. The safety

Table 1 Quantification results of PET imaging and biodistribution studies of ^{64}Cu -DOTA-PSMA-3Q and ^{64}Cu -NOTA-PSMA-3Q. Health organization data from biodistribution study; tumor and Tumor/Muscle data from PET imaging. Data is presented as Mean \pm SD) (% ID/g)

Organ	^{64}Cu -DOTA-PSMA-3Q				^{64}Cu -NOTA-PSMA-3Q			
	1 h	4 h	12 h	24 h	1 h	4 h	12 h	24 h
Blood	0.62 ± 0.19	0.42 ± 0.08	0.37 ± 0.01	0.30 ± 0.06	0.36 ± 0.07	0.19 ± 0.01	0.13 ± 0.00	0.11 ± 0.02
Brain	0.07 ± 0.03	0.07 ± 0.00	0.09 ± 0.01	0.08 ± 0.02	0.03 ± 0.01	0.03 ± 0.01	0.03 ± 0.00	0.03 ± 0.00
Liver	2.92 ± 0.44	2.47 ± 0.28	1.71 ± 0.04	1.14 ± 0.29	0.83 ± 0.06	0.58 ± 0.14	0.31 ± 0.04	0.29 ± 0.13
Spleen	1.28 ± 0.44	0.90 ± 0.31	0.81 ± 0.33	0.56 ± 0.33	0.73 ± 0.25	0.44 ± 0.14	0.16 ± 0.03	0.13 ± 0.06
Kidney	59.79 ± 3.18	3.65 ± 1.05	1.42 ± 0.20	0.92 ± 0.20	27.25 ± 7.55	1.10 ± 0.21	0.35 ± 0.02	0.22 ± 0.03
Stomach	1.48 ± 0.79	1.14 ± 0.62	0.49 ± 0.08	0.49 ± 0.09	0.22 ± 0.04	0.23 ± 0.08	0.14 ± 0.02	0.15 ± 0.07
Intestine	1.82 ± 0.57	0.87 ± 0.69	0.70 ± 0.29	0.70 ± 0.12	0.25 ± 0.06	0.29 ± 0.11	0.26 ± 0.01	0.22 ± 0.05
Heart	0.96 ± 0.46	0.65 ± 0.07	0.66 ± 0.09	0.52 ± 0.05	0.18 ± 0.03	0.15 ± 0.03	0.14 ± 0.00	0.14 ± 0.03
Lung	1.84 ± 0.77	1.11 ± 0.10	0.96 ± 0.30	0.83 ± 0.32	0.52 ± 0.03	0.27 ± 0.09	0.28 ± 0.02	0.18 ± 0.04
Bone	0.57 ± 0.16	0.46 ± 0.02	0.47 ± 0.06	0.41 ± 0.08	0.36 ± 0.03	0.33 ± 0.06	0.33 ± 0.04	0.33 ± 0.01
Muscle	0.27 ± 0.07	0.18 ± 0.02	0.14 ± 0.01	0.16 ± 0.00	0.13 ± 0.02	0.07 ± 0.01	0.07 ± 0.02	0.09 ± 0.00
Tumor	8.64 ± 1.39	9.56 ± 1.71	9.80 ± 0.65	10.05 ± 0.46	8.22 ± 0.73	7.41 ± 1.01	6.55 ± 1.29	5.38 ± 1.06
Tumor/Muscle	8.39 ± 0.13	8.94 ± 1.19	10.22 ± 0.29	7.88 ± 1.41	24.06 ± 4.57	25.87 ± 5.72	19.78 ± 2.67	15.44 ± 2.08

of ^{64}Cu -DOTA-PSMA-3Q has been confirmed in previous studies [17].

The biodistribution of ^{64}Cu -NOTA-PSMA-3Q and ^{64}Cu -DOTA-PSMA-3Q in healthy BALB/c male mice is presented in Table 1. Both tracers exhibited rapid clearance from the blood, with radioactivity levels at 1-hour post-injection measured at $0.36 \pm 0.07\%$ ID/g for ^{64}Cu -NOTA-PSMA-3Q and $0.62 \pm 0.19\%$ ID/g for ^{64}Cu -DOTA-PSMA-3Q, indicating faster blood clearance for the former. Liver uptake was significantly higher for ^{64}Cu -DOTA-PSMA-3Q compared to ^{64}Cu -NOTA-PSMA-3Q ($2.92 \pm 0.44\%$ ID/g vs. $0.83 \pm 0.06\%$ ID/g, $P=0.027$), suggesting that ^{64}Cu -NOTA-PSMA-3Q may exhibit lower hepatobiliary excretion. Spleen uptake was also higher for ^{64}Cu -DOTA-PSMA-3Q ($1.28 \pm 0.44\%$ ID/g) than for ^{64}Cu -NOTA-PSMA-3Q ($0.73 \pm 0.25\%$ ID/g), but this difference did not reach statistical significance ($P=0.134$). Both tracers showed high initial kidney uptake, which decreased significantly over 24 h. For ^{64}Cu -DOTA-PSMA-3Q, kidney uptake declined from $59.79 \pm 3.18\%$ ID/g to $0.92 \pm 0.20\%$ ID/g, while for ^{64}Cu -NOTA-PSMA-3Q, uptake decreased from $27.25 \pm 7.55\%$ ID/g to $0.22 \pm 0.03\%$ ID/g, demonstrating rapid renal clearance for both tracers. Furthermore, ^{64}Cu -NOTA-PSMA-3Q exhibited lower accumulation in the lungs, stomach, and intestines compared to ^{64}Cu -DOTA-PSMA-3Q, while other organs

showed minimal radioactive accumulation and rapid clearance, highlighting the favorable pharmacokinetic profile of ^{64}Cu -NOTA-PSMA-3Q.

The Micro-PET imaging of 22RV1 tumor-bearing mice, as depicted in Fig. 1, revealed notable uptake of both ^{64}Cu -NOTA-PSMA-3Q and ^{64}Cu -DOTA-PSMA-3Q tracers within tumor tissues. Following intravenous administration, the temporal tracer uptake was quantified as follows: at 1 h, uptake was $8.22 \pm 0.73\%$ ID/g for ^{64}Cu -NOTA-PSMA-3Q and $8.64 \pm 1.39\%$ ID/g for ^{64}Cu -DOTA-PSMA-3Q ($P=0.669$); at 4 h, uptake was $7.41 \pm 1.01\%$ ID/g versus $9.56 \pm 1.71\%$ ID/g ($P=0.134$); at 12 h, it was $6.55 \pm 1.29\%$ ID/g versus $9.80 \pm 0.65\%$ ID/g ($P=0.018$); and at 24 h, uptake decreased to $5.38 \pm 1.06\%$ ID/g versus $10.05 \pm 0.46\%$ ID/g ($P=0.002$), respectively. Additionally, the tumor-to-muscle ratio for ^{64}Cu -NOTA-PSMA-3Q was significantly higher across all measured time points, with values of 24.06 ± 4.57 at 1 h, 25.87 ± 5.729 at 4 h, 19.78 ± 2.67 at 12 h, and 15.44 ± 2.08 at 24 h. In contrast, the tumor-to-muscle ratios for ^{64}Cu -DOTA-PSMA-3Q were consistently lower, recorded as 8.39 ± 0.13 , 8.94 ± 1.19 , 10.22 ± 0.29 , and 7.88 ± 1.41 at the respective time points. The differences in tumor-to-muscle ratios between the two tracers were statistically significant at all time points ($P<0.05$). One-hour post-injection, liver uptake of ^{64}Cu -DOTA-PSMA-3Q was notably higher than that of ^{64}Cu -NOTA-PSMA-3Q, with

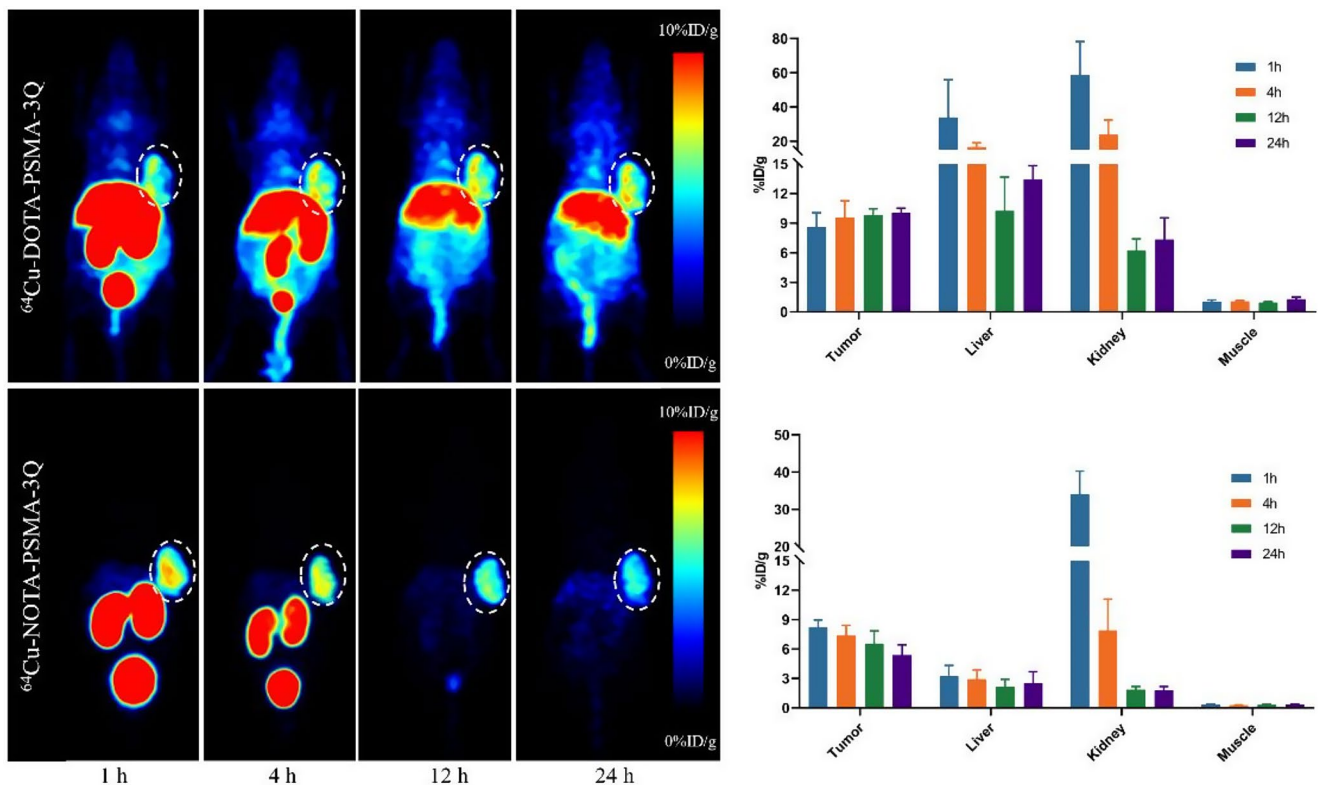


Fig. 1 Representative static PET imaging and quantification results in 22RV1 tumor-bearing mice with ^{64}Cu -NOTA-PSMA-3Q and ^{64}Cu -DOTA-PSMA-3Q

uptake values of $24.00 \pm 4.73\%$ ID/g and $3.28 \pm 1.04\%$ ID/g, respectively, representing a 7.27-fold increase for ^{64}Cu -DOTA-PSMA-3Q. This observation was consistent with the biodistribution data, which also highlighted significant tracer accumulation in the kidneys and bladder, while only minimal radioactivity was observed in other normal tissues. These findings underscore the superior tumor selectivity of ^{64}Cu -NOTA-PSMA-3Q over ^{64}Cu -DOTA-PSMA-3Q and highlight its potential as a more favorable imaging agent for PSMA-expressing tumors.

Preliminary clinical PET/CT imaging in humans

The preliminary clinical research, approved by the Ethics Committee of the First Medical Center of the People's Liberation Army General Hospital, was conducted from May 2023 to May 2024. The study enrolled a total of 23 patients suspected of having prostate cancer (PCa), with 12 patients undergoing ^{64}Cu -NOTA-PSMA-3Q PET/CT scans and 11 patients undergoing ^{64}Cu -DOTA-PSMA-3Q PET/CT scans. No adverse reactions or significant changes in vital signs were reported during any of the PET/CT imaging sessions, indicating good tolerability and safety of both tracers. Of the 23 participants, 18 underwent biopsy procedures, resulting in 15 pathological confirmations of PCa

and 3 diagnoses of benign prostatic hyperplasia (BPH). An additional 5 patients were confirmed to have PCa through follow-up evaluations, bringing the total number of confirmed PCa cases to 20 patients. Among these cases, 10 were imaged with ^{64}Cu -NOTA-PSMA-3Q and 10 with ^{64}Cu -DOTA-PSMA-3Q, ensuring an equal distribution of PCa cases across the two imaging groups. The analysis of tumor burden and tumor lesion uptake values, detailed in Table 2, revealed that the mean maximum standardized uptake values (SUVmax) for primary tumor detection were 18.89 ± 7.38 for ^{64}Cu -NOTA-PSMA-3Q and 19.54 ± 10.65 for ^{64}Cu -DOTA-PSMA-3Q. These findings underscore the diagnostic utility of both tracers for the detection of PCa, with comparable SUVmax values observed between the two imaging agents.

The representative maximum intensity projection images of the two radiopharmaceuticals are illustrated in Figs. 2 and 3. The range and mean of the maximum standardized uptake value (SUVmax) for the primary organs of the patients are summarized in Table 3. As depicted in the figure, both radiopharmaceuticals are predominantly excreted via the kidneys. While both radiopharmaceuticals exhibit high activity in organs with elevated PSMA expression (e.g., lacrimal glands, parotid glands, submandibular glands, sublingual glands, and kidneys), a notable distinction is observed: the

Table 2 Individual patient characteristics and tumor lesion uptake

Patient No	Age	PSA(ng/mL)	Primary tumor (SUVmax)	Lymph node metastases (SUVmax)	Bone metastases (SUVmax)	Gleason score	^{64}Cu -NOTA-PSMA-3Q(NOTA) or ^{64}Cu -DOTA-PSMA-3QDOTA
1	71	10.00	42.68	None	None	4+3	NOTA
2	81	21.34	6.40	None	None	None	NOTA
3	76	41.63	54.15	None	None	4+4	NOTA
4	70	21.28	19.92	None	None	4+3	NOTA
5	65	18.49	14.46	None	None	4+3	NOTA
6	79	50.00	9.51	None	None	3+4	NOTA
7	67	21.25	13.37	None	None	None	NOTA
8	67	8.52	6.08	None	None	3+3	NOTA
9	67	21.31	27.64	5.26–27.05	3.83–33.54	None	NOTA
10	65	15.15	NE	None	None	None	NOTA
11	68	5.00	10.82	None	None	None	NOTA
12	80	10.30	14.87	None	None	4+3	DOTA
13	69	15.06	40.19	None	None	4+3	DOTA
14	70	23.10	54.65	None	None	4+3	DOTA
15	65	15.43	12.30	None	None	4+3	DOTA
16	67	9.71	22.47	None	None	3+4	DOTA
17	76	23.14	24.58	None	None	3+5	DOTA
18	68	45.12	24.46	None	None	4+3	DOTA
19	66	18.23	29.29	None	None	4+4	DOTA
20	65	18.12	27.64	None	None	None	DOTA
21	72	18.26	NE	None	None	None	DOTA
22	84	4.58	7.99	None	None	3+4	DOTA
23	61	12.46	NE	None	None	None	DOTA

NE: Negative expression

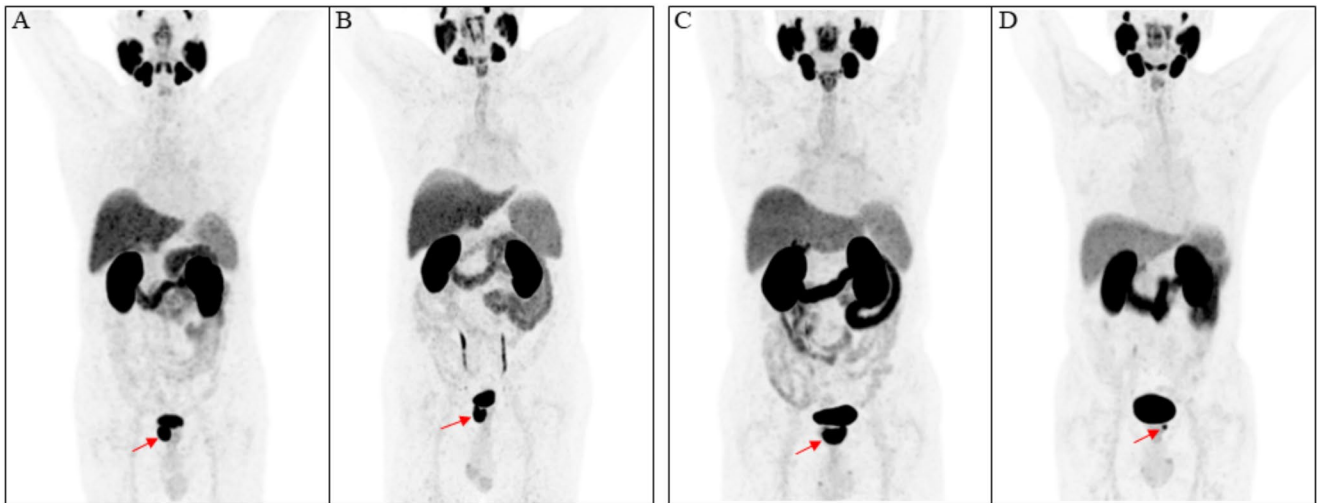


Fig. 2 Shows the representative maximum intensity PET/CT projection images of ^{64}Cu -DOTA-PSMA-3Q (A, B) and ^{64}Cu -NOTA-PSMA-3Q (C, D) in prostate cancer patients 2 h after injection. A: Male, 70 years old, PSA=23.1 ng/mL, lacrimal gland (SUVmax=13.56), parotid gland (SUVmax=21.004), submandibular gland (SUVmax=19.406), liver (SUVmax=11.084), spleen (SUVmax=6.239), primary lesion (SUVmax=54.65). B: Male, 68 years old, PSA=45.12 ng/mL, lacrimal gland (SUVmax=14.38), parotid gland (SUVmax=18.21), submandibular gland (SUVmax=17.19), liver (SUVmax=9.045),

spleen (SUVmax=5.99), primary lesion (SUVmax=24.46). C: Male, 70 years old, 65 kg, PSA=21.28 ng/mL, lacrimal gland (SUVmax=11.74), parotid gland (SUVmax=15.12), submandibular gland (SUVmax=18.25), liver (SUVmax=3.86), spleen (SUVmax=3.35), primary lesion (SUVmax=19.92). D: Male, 68 years old, 59 kg, PSA=5.00 ng/mL, lacrimal gland (SUVmax=21.11), parotid gland (SUVmax=26.46), submandibular gland (SUVmax=29.07), liver (SUVmax=5.01), spleen (SUVmax=4.57), primary lesion (SUVmax=10.82). The red arrow shows the tumor

uptake of ^{64}Cu -NOTA-PSMA-3Q is higher in the lacrimal glands (17.73 vs. 10.84), parotid glands (20.98 vs. 16.30), and submandibular glands (20.26 vs. 17.28) compared to ^{64}Cu -DOTA-PSMA-3Q, whereas the uptake in the sublingual glands is lower (7.10 vs. 7.49). In the liver, which is of particular interest, the uptake of ^{64}Cu -NOTA-PSMA-3Q is significantly lower than that of ^{64}Cu -DOTA-PSMA-3Q (4.04 vs. 8.18). Additionally, the uptake of ^{64}Cu -NOTA-PSMA-3Q in the brain, lungs, and muscles is also lower than that of ^{64}Cu -DOTA-PSMA-3Q (0.12 vs. 0.28), (0.47 vs. 0.65), and (0.52 vs. 0.79), respectively. No statistically significant differences were observed in the uptake of the two radiopharmaceuticals in other normal human organs.

Discussion

In this study, we conducted a preliminary investigation using PET/CT imaging to assess the performance of ^{64}Cu conjugated with PSMA-3Q via the NOTA chelator (^{64}Cu -NOTA-PSMA-3Q). We specifically focused on comparing the in vivo biodistribution differences between PSMA-3Q labeled with two bifunctional chelators, DOTA and NOTA.

^{64}Cu has emerged as a highly effective PET imaging radionuclide, offering unique advantages in diagnostic imaging and therapeutic applications. Recent advancements have led to the development of several ^{64}Cu -labeled PSMA

radiotracers [19–22], which have shown significant potential for the early detection of recurrent disease and local recurrences [23]. One of the most noteworthy benefits of ^{64}Cu is its role in the theranostic pair ($^{64}\text{Cu}/^{67}\text{Cu}$), which enables a dual diagnostic-therapeutic approach. As a diagnostic agent, ^{64}Cu provides critical information for precision oncology, while ^{67}Cu serves as a therapeutic radioisotope, making this pairing particularly valuable in personalized medicine. The physical properties of ^{64}Cu further enhance its utility in PET imaging. Its extended half-life allows imaging at later time points, improving the delineation of tumors with greater accuracy and detail. This feature also facilitates the decentralized production and distribution of radiotracers, reducing logistical constraints on production sites [15]. Another unique advantage of ^{64}Cu -labeled PSMA-targeted agents is the ability to incorporate ^{67}Cu for therapeutic purposes within the same compound. This capability streamlines the transition from imaging to treatment, thereby supporting the development of dual-function theranostic agents. Despite the growing interest in ^{67}Cu , its availability is currently more limited compared to the widely used ^{177}Lu . However, efforts are underway to enhance global access to ^{67}Cu [24]. Given its shorter half-life of 2.58 days relative to ^{177}Lu 's 6.7 days, ^{67}Cu is particularly suited for pharmacokinetic studies of peptide-based drugs that are rapidly excreted [25]. Efficient chelation is essential for ensuring the stability and efficacy of radiotracers. Among available chelators, DOTA and NOTA are widely regarded as effective for various

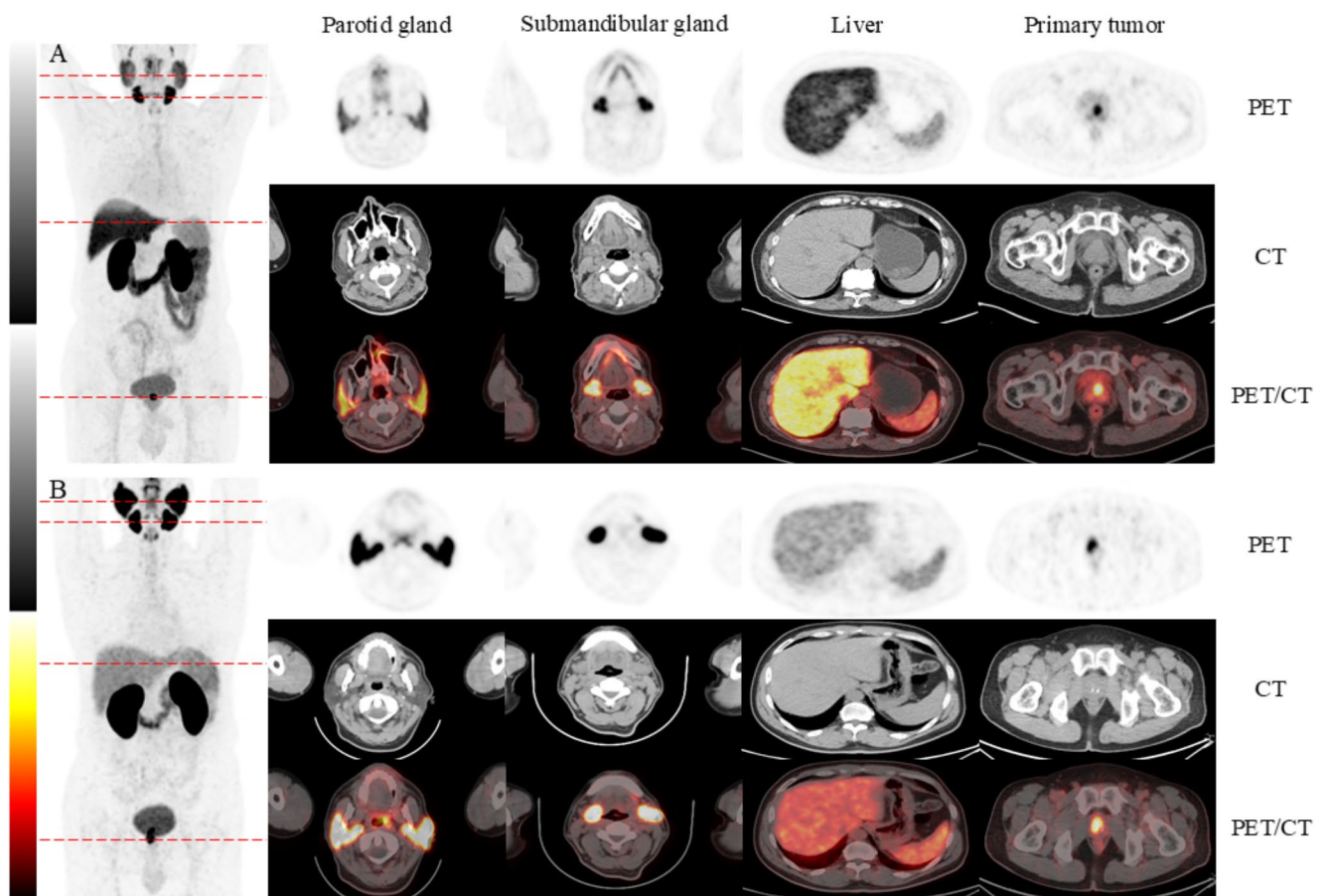


Fig. 3 The MIP image, low-dose axial CT image, and fused PET/CT image (A) of patient no. 12 at 2 h post-injection of ^{64}Cu -DOTA-PSMA-3Q in an 80-year-old primary PCa patient with a rising PSA level of 10.3 ng/mL and a Gleason score of 4+3=7. From left to right, they are the parotid gland (SUVmax=7.49), submandibular gland (SUVmax=12.97), liver (SUVmax=8.09), spleen (SUVmax=4.36), and primary lesion (SUVmax=14.87). The MIP image, low-dose axial CT

image, and fused PET/CT image (B) of patient no. 5 at 2 h post-injection of ^{64}Cu -NOTA-PSMA-3Q in a 65-year-old primary PCa patient with a rising PSA level of 18.49 ng/mL and a Gleason score of 4+3=7. From left to right, they are the parotid gland (SUVmax=19.83), submandibular gland (SUVmax=24.97), liver (SUVmax=4.57), spleen (SUVmax=4.76), and primary lesion (SUVmax=14.46)

Table 3 The SUVmax of ^{64}Cu -NOTA-PSMA-3Q and ^{64}Cu -DOTA-PSMA-3Q imaging in various human organs

Organ	^{64}Cu -NOTA-PSMA-3Q(n=11)		^{64}Cu -DOTA-PSMA-3Q(n=12)		P value
	Average	Range	Average	Range	
Lacrimal Gland	17.73	11.35–24.48	10.84	5.35–16.00	<0.001
Parotid Gland	20.98	13.37–38.63	16.30	7.49–21.82	0.064
Submandibular Gland	20.26	14.26–29.07	17.28	12.39–24.32	0.140
Sublingual Gland	7.10	4.27–15.71	7.49	3.12–14.97	0.801
Brain	0.12	0.04–0.32	0.28	0.08–0.61	0.009
Heart	1.23	0.84–1.59	1.51	1.18–1.82	0.004
Liver	4.04	2.94–5.01	8.18	5.99–11.08	<0.001
Spleen	4.75	3.12–7.64	5.96	3.88–9.72	0.093
Lung	0.47	0.30–0.76	0.65	0.52–0.99	0.007
Stomach	1.48	0.94–2.18	1.54	0.88–2.05	0.713
Intestine	5.73	1.56–13.87	5.45	2.75–9.84	0.848
Kidney	43.95	25.04–67.10	41.69	20.27–74.10	0.738
Bone	0.45	0.12–1.07	0.45	0.31–0.93	0.993
Muscle	0.52	0.34–0.95	0.79	0.57–1.09	0.001

radionuclides due to their favorable geometry and thermodynamically stable metal-binding sites. DOTA is considered the “gold standard” chelator, capable of forming stable complexes with a broad spectrum of isotopes, such as ^{225}Ac , $^{86/90}\text{Y}$, ^{177}Lu , ^{111}In , and $^{44/47}\text{Sc}$ [26]. Its versatility makes it the preferred choice for chelating isotopes used in both imaging and radioligand therapy.

However, specific challenges arise when DOTA is used with ^{64}Cu . One of the primary issues is the high liver and gallbladder uptake observed with ^{64}Cu -labeled compounds. Research suggests that this uptake is caused by the dissociation of copper from its chelator, which is mediated by the action of superoxide dismutase (SOD) in the liver [27]. This dissociation leads to the redistribution of free copper ions, contributing to higher off-target activity. While DOTA maintains good stability with other isotopes, its *in vivo* kinetic stability with ^{64}Cu is relatively lower compared to NOTA.

NOTA, on the other hand, offers a more stable chelation for ^{64}Cu . Its superior kinetic stability minimizes copper release, leading to reduced hepatic uptake. For imaging applications where minimizing radiation dose to the liver is a priority, NOTA is the preferred chelator for ^{64}Cu -based radiopharmaceuticals. However, for therapeutic purposes—especially when working with isotopes that require extended stability, such as ^{90}Y or ^{177}Lu —DOTA is more appropriate due to its ability to maintain long-term complexation [11]. The choice of chelator, therefore, depends on the specific clinical objective: if liver sparing and reduced background uptake are essential, NOTA should be used. Conversely, for radioligand therapy, where isotopes must remain bound for longer durations, DOTA remains the preferred choice.

In this study, both DOTA and NOTA were demonstrated to be effective bifunctional chelating agents (BFCAs) for the preparation of ^{64}Cu -labeled PSMA radiopharmaceuticals used in PET/CT imaging of prostate cancer patients. However, a key distinction was observed: ^{64}Cu -NOTA-PSMA-3Q exhibited significantly lower liver uptake compared to ^{64}Cu -DOTA-PSMA-3Q, consistent with prior studies that have directly compared these chelators [28]. This reduction in hepatic uptake is clinically relevant, as it enhances image clarity by reducing background signal, thereby facilitating the detection of liver lesions.

The enhanced *in vivo* stability of ^{64}Cu -NOTA-PSMA-3Q can be attributed to the chelation properties of NOTA. Previous studies have established that ^{64}Cu -NODAGA-PSMA ligands exhibit greater stability than their DOTA-based counterparts, leading to improved diagnostic performance characterized by higher tumor-to-background ratios. Comparative analyses have shown that NOTA provides superior stability for ^{64}Cu -labeled compounds compared to DOTA [29]. This increased stability is likely due to the smaller

cavity size of NOTA relative to DOTA [30], which allows for a more tightly bound copper complex, thereby minimizing dissociation and off-target uptake.

From a clinical perspective, the reduced liver uptake of ^{64}Cu -NOTA-PSMA-3Q has significant implications for prostate cancer imaging, particularly in patients with suspected liver metastases. Visceral metastases, especially in the liver, are known to be strong predictors of poor progression-free survival (PFS) and increased mortality risk [31]. As a result, the ability of ^{64}Cu -NOTA-PSMA-3Q to provide clear, high-contrast imaging of the liver may improve the early detection and localization of metastatic lesions. This advantage could play a critical role in patient management by enabling more accurate staging and facilitating timely therapeutic intervention. Hence, ^{64}Cu -NOTA-PSMA-3Q offers a clinically valuable diagnostic tool for the assessment of prostate cancer with potential liver involvement, supporting more precise and individualized patient care.

This study identified significant differences in the uptake of ^{64}Cu -labeled compounds in organs with high PSMA expression, including the lacrimal, parotid, and submandibular glands. Notably, the uptake of ^{64}Cu -labeled DOTA in these glands was substantially lower than that of ^{64}Cu -labeled NOTA. This finding aligns with prior research by Niels J. Rupp et al. (2019), who observed that the accumulation of PSMA-targeted radiopharmaceuticals in salivary gland tissue is predominantly nonspecific [32]. Understanding the mechanisms behind this differential uptake is critical for the future design of PSMA-targeted radiopharmaceuticals, particularly in therapies using α -particle emitters with high linear energy transfer (LET). The notable difference in salivary gland uptake between ^{64}Cu -DOTA and ^{64}Cu -NOTA may be attributed, in part, to the pH environment of the saliva, which typically ranges from 6.5 to 7 [33]. The kinetic stability of copper chelates is known to be pH-dependent, with studies showing that Cu-NOTA exhibits greater stability than Cu-DOTA at a pH of 4.6 [11]. However, at the neutral pH found in saliva, DOTA may provide a more stable binding environment for copper, potentially resulting in reduced dissociation and uptake in the salivary glands. This pH-driven stability difference offers a plausible explanation for the observed disparity in glandular uptake between ^{64}Cu -DOTA and ^{64}Cu -NOTA.

From a clinical perspective, the accumulation of PSMA-targeted radiopharmaceuticals in the salivary glands has significant implications for patient well-being, particularly in the context of radionuclide therapy. Radiation-induced damage to salivary glands can result in xerostomia (dry mouth), a debilitating side effect that significantly impacts quality of life [34]. While xerostomia induced by β -emitting radionuclides like ^{177}Lu is often reversible, irreversible gland damage has been reported with α -emitters such as ^{225}Ac [35].

This irreversible damage poses a major challenge for dose escalation in PSMA-targeted radioligand therapy (RLT) for prostate cancer. Given these concerns, DOTA may be the preferred chelator over NOTA in therapies involving α -emitting nuclides, as its lower uptake in salivary glands could reduce the risk of radiation-induced xerostomia. For future clinical applications, particularly in intravenous radionuclide irradiation therapy, DOTA may offer a safer option when using ^{64}Cu as the therapeutic radionuclide. By limiting uptake in non-target organs like the salivary glands, DOTA-labeled PSMA-targeted radiopharmaceuticals may enable higher therapeutic doses while mitigating adverse effects. Interestingly, the higher uptake of NOTA-labeled ligands in salivary glands may present a potential advantage for targeting tumors that originate or metastasize to these glands [36]. This dual role highlights the need for more targeted strategies to balance effective tumor targeting with reduced off-target toxicity. Further studies are required to better understand the mechanisms driving salivary gland uptake and to explore potential solutions for mitigating toxicity. These efforts are crucial for optimizing PSMA-targeted RLT protocols, particularly in patients with prostate cancer who are at risk of xerostomia due to salivary gland irradiation.

It is noteworthy that the uptake of ^{64}Cu -NOTA-PSMA-3Q and ^{64}Cu -DOTA-PSMA-3Q in the brain is minimal, a finding that aligns with the known properties of PSMA radioligands. This minimal uptake can be attributed to the molecular weight of PSMA, which, without the radionuclide label, ranges from 400 to 500 Da. This exceeds the typical mass transport limit of the blood-brain barrier, thereby restricting its passive diffusion into the brain. As a result, any detectable brain uptake of ^{64}Cu -PSMA could be indicative of a disruption or compromise in blood-brain barrier integrity [23]. Despite the valuable insights provided by this study, certain limitations must be acknowledged. The most prominent limitation is the relatively small sample size, which calls for further validation using a larger cohort to confirm the generalizability of these findings. Expanding the sample size would increase the statistical power and provide a more comprehensive understanding of the biodistribution and pharmacokinetics of ^{64}Cu -NOTA-PSMA-3Q and ^{64}Cu -DOTA-PSMA-3Q. Another key limitation is the absence of biodistribution data from healthy volunteers. While patient-based studies are often more reflective of real-world clinical conditions, the inclusion of healthy volunteers could offer critical baseline data for comparison. Establishing a healthy biodistribution profile for these radiopharmaceuticals would provide context for interpreting patient results, particularly when assessing potential variations in uptake caused by disease-related changes, such as alterations in PSMA expression or blood-brain barrier integrity.

Future research should consider the inclusion of healthy volunteer data to enhance the robustness of study conclusions and enable a more holistic assessment of the biodistribution patterns of ^{64}Cu -labeled PSMA radiopharmaceuticals.

Conclusion

In summary, this study confirmed that both NOTA and DOTA are effective chelating agents for ^{64}Cu -labeled PSMA-3Q in PET/CT imaging. Each chelator exhibited distinct biodistribution characteristics, with ^{64}Cu -NOTA-PSMA-3Q showing significantly lower uptake in the liver compared to ^{64}Cu -DOTA-PSMA-3Q. Conversely, ^{64}Cu -DOTA-PSMA-3Q demonstrated reduced uptake in the salivary glands relative to ^{64}Cu -NOTA-PSMA-3Q. These findings highlight the differential kinetic stability and biodistribution properties of the two chelators, which may have important implications for selecting the optimal chelator based on the specific clinical objectives of PET imaging or radionuclide therapy.

Supplementary Information The online version contains supplementary material available at <https://doi.org/10.1007/s00259-025-07131-3>.

Author contributions Conceptualization: Jinming Zhang, Yachao Liu, Ruimin Wang; Methodology: Xiaojun Zhang, Huanhuan Liu and Jinming Zhang; Formal analysis and investigation: Huanhuan Liu, Xiaojun Zhang, Jingfeng Zhang, Yue Pan, Hui Wen, Xiaodan Xu, Shina Wu, Yuan Wang, Cong Zhang, Guangyu Ma; Writing - original draft preparation: Huanhuan Liu; Writing - review and editing: Jinming Zhang; Supervision: Yachao Liu, Ruimin Wang, Jinming Zhang.

Funding No funding was received for conducting this study.

Data availability Data are available for legitimate researchers who request it from the authors. 1.

Declarations

Ethical approval This study was approved by the Ethics Committee of Chinese PLA General Hospital (approval of No. S2023-208-02, Registration number of ChiCTR2300072655).

Consent to participate Informed consent was obtained from all individual participants included in the study.

Consent to publish All authors have read this manuscript and would like to have it considered exclusively for publication.

Competing interests The authors have no competing interests to declare that are relevant to the content of this article.

Open Access This article is licensed under a Creative Commons Attribution-NonCommercial-NoDerivatives 4.0 International License, which permits any non-commercial use, sharing, distribution and reproduction in any medium or format, as long as you give appropriate credit to the original author(s) and the source, provide a link to the

Creative Commons licence, and indicate if you modified the licensed material. You do not have permission under this licence to share adapted material derived from this article or parts of it. The images or other third party material in this article are included in the article's Creative Commons licence, unless indicated otherwise in a credit line to the material. If material is not included in the article's Creative Commons licence and your intended use is not permitted by statutory regulation or exceeds the permitted use, you will need to obtain permission directly from the copyright holder. To view a copy of this licence, visit <http://creativecommons.org/licenses/by-nc-nd/4.0/>.

References

- Wang L, Lu B, He M, et al. Prostate cancer incidence and mortality: global status and temporal trends in 89 countries from 2000 to 2019. *Front Public Health*. 2022;10. <https://doi.org/10.3389/fpubh.2022.811044>.
- Sung H, Ferlay J, Siegel RL, et al. Global cancer statistics 2020: Globocan estimates of incidence and mortality worldwide for 36 cancers in 185 countries. *CA: A Cancer J Clin*. 2021;71(3):209–49. <https://doi.org/10.3322/caac.21660>.
- Fendler WP, Calais J, Eiber M, et al. Assessment of 68ga-psma-11 pet accuracy in localizing recurrent prostate cancer. *JAMA Oncol*. 2019;5(6). <https://doi.org/10.1001/jamaoncol.2019.0096>.
- Hofman MS, Lawrentschuk N, Francis RJ, et al. Prostate-specific membrane antigen pet-ct in patients with high-risk prostate cancer before curative-intent surgery or radiotherapy (prospma): a prospective, randomised, multicentre study. *Lancet*. 2020;395(10231):1208–16. [https://doi.org/10.1016/s0140-6736\(20\)30314-7](https://doi.org/10.1016/s0140-6736(20)30314-7).
- Fendler WP, Eiber M, Beheshti M, et al. Psma pet/ct: joint eann procedure guideline/snm procedure standard for prostate cancer imaging 2.0. *Eur J Nucl Med Mol Imaging*. 2023;50(5):1466–86. <https://doi.org/10.1007/s00259-022-06089-w>.
- Mena E, Lindenberg L, Choyke PL. Update on psma-based prostate cancer imaging. *Semin Nucl Med*. 2024. <https://doi.org/10.1053/j.semnuclmed.2024.10.004>.
- Meher N, Vanbroeklin HF, Wilson DM, et al. Psma-targeted nanotheranostics for imaging and radiotherapy of prostate cancer. *Pharmaceuticals*. 2023;16(2). <https://doi.org/10.3390/ph16020315>.
- Milot M-C, Benesty OB, Dumulon-Perreault V, et al. 64cu-dotha2-psma, a novel psma pet radiotracer for prostate cancer with a long imaging time window. *Pharmaceuticals*. 2022;15(8). <https://doi.org/10.3390/ph15080996>.
- Krasnovskaya OO, Abramchuck D, Erofeev A, et al. Recent advances in 64cu/67cu-based radiopharmaceuticals. *Int J Mol Sci*. 2023;24(11). <https://doi.org/10.3390/ijms24119154>.
- Nelson BJB, Leier S, Wilson J, et al. 64cu production via the 68zn(p,n α)64cu nuclear reaction: an untapped, cost-effective and high energy production route. *Nucl Med Biol*. 2024;128–129:108875. <https://doi.org/10.1016/j.nucmedbio.2024.108875>.
- Lee I, Kim MH, Lee K, et al. Comparison of the effects of dota and nota chelators on 64cu-cudotadipep and 64cu-cunotadipep for prostate cancer. *Diagnostics*. 2023;13(16). <https://doi.org/10.3390/diagnostics13162649>.
- Liu Z, Li Z-B, Cao Q, et al. Small-animal pet of tumors with 64cu-labeled rgd-bombesin heterodimer. *J Nucl Med*. 2009;50(7):1168–77. <https://doi.org/10.2967/jnumed.108.061739>.
- Yang H, Gao F, Mcneil B, et al. Synthesis of dota-pyridine chelates for 64cu coordination and radiolabeling of α msH peptide. *EJNMMI Radiopharmacy Chem*. 2021;6(1):3. <https://doi.org/10.1186/s41181-020-00119-4>.
- Chen X, Niu W, Du Z, et al. 64cu radiolabeled nanomaterials for positron emission tomography (pet) imaging. *Chin Chem Lett*. 2022;33(7):3349–60. <https://doi.org/10.1016/j.cclet.2022.02.070>.
- Carlos Dos Santos J, Beijer B, Bauder-Wüst U, et al. Development of novel psma ligands for imaging and therapy with copper isotopes. *J Nucl Med*. 2020;61(1):70–9. <https://doi.org/10.2967/jnumed.119.229054>.
- Malmberg J, Perols A, Varasteh Z, et al. Comparative evaluation of synthetic anti-her2 affibody molecules site-specifically labelled with 111in using n-terminal dota, nota and nodaga chelators in mice bearing prostate cancer xenografts. *Eur J Nucl Med Mol Imaging*. 2011;39(3):481–92. <https://doi.org/10.1007/s00259-011-1992-9>.
- Zhang J, Niu S, Liu Y, et al. Real-time diagnosis of sampled lesions in targeted biopsy of prostate cancer using a novel tracer [64cu] cu-dota-psma-3q: a pilot preclinical study. *Eur J Nucl Med Mol Imaging*. 2024. <https://doi.org/10.1007/s00259-024-07000-5>.
- Wu Y, Zhang X, Zhou H, et al. Synthesis, preclinical evaluation, and first-in-human study of all8f-psma-q for prostate cancer imaging. *Eur J Nucl Med Mol Imaging*. 2022;49(8):2774–85. <https://doi.org/10.1007/s00259-022-05775-z>.
- Banerjee SR, Pullambhatla M, Foss CA, et al. 64cu-labeled inhibitors of prostate-specific membrane antigen for pet imaging of prostate cancer. *J Med Chem*. 2014;57(6):2657–69. <https://doi.org/10.1021/jm401921j>.
- Hagemeyer CE, Gourni E, Canovas C, et al. (r)-nodaga-psma: a versatile precursor for radiometal labeling and nuclear imaging of psma-positive tumors. *PLoS ONE*. 2015;10(12). <https://doi.org/10.1371/journal.pone.0145755>.
- Alberts IL, Seide SE, Mingels C, et al. Comparing the diagnostic performance of radiotracers in recurrent prostate cancer: a systematic review and network meta-analysis. *Eur J Nucl Med Mol Imaging*. 2021;48(9):2978–89. <https://doi.org/10.1007/s00259-021-05210-9>.
- Liu T, Liu C, Zhang Z, et al. 64cu-psma-bch: a new radiotracer for delayed pet imaging of prostate cancer. *Eur J Nucl Med Mol Imaging*. 2021;48(13):4508–16. <https://doi.org/10.1007/s00259-021-05426-9>.
- Calabria F, Pichler R, Leporace M, et al. 68ga/64cu psma bio-distribution in prostate cancer patients: potential pitfalls for different tracers. *Curr Radiopharmaceuticals*. 2019;12(3):238–46. <https://doi.org/10.2174/1874471012666190515090755>.
- Mou L, Martini P, Pupillo G, et al. 67cu production capabilities: a mini review. *Molecules*. 2022;27(5). <https://doi.org/10.3390/molecules27051501>.
- Huynh TT, Van Dam EM, Sreekumar S, et al. Copper-67-labeled bombesin peptide for targeted radionuclide therapy of prostate cancer. *Pharmaceuticals*. 2022;15(6). <https://doi.org/10.3390/ph15060728>.
- Price EW, Orvig C. Matching chelators to radiometals for radiopharmaceuticals. *Chem Soc Rev*. 2014;43(1):260–90. <https://doi.org/10.1039/c3cs60304k>.
- Sprague JE, Peng Y, Sun X, et al. Preparation and biological evaluation of copper-64-labeled tyr3-octreotate using a cross-bridged macrocyclic chelator. *Clin Cancer Res*. 2004;10(24):8674–82. <https://doi.org/10.1158/1078-0432.Ccr-04-1084>.
- Sevcenco S, Klingler HC, Eredics K, et al. Application of cu-64 nodaga-psma pet in prostate cancer. *Adv Therapy*. 2018;35(6):779–84. <https://doi.org/10.1007/s12325-018-0711-3>.
- Bachmann MP, Zhang Y, Hong H, et al. Positron emission tomography imaging of cd105 expression with a 64cu-labeled monoclonal antibody: Nota is superior to dota. *PLoS ONE*. 2011;6(12). <https://doi.org/10.1371/journal.pone.0028005>.

30. Guleria M, Das T, Amirdhanayagam J, et al. Comparative evaluation of using nota and dota derivatives as bifunctional chelating agents in the preparation of 68ga-labeled porphyrin: impact on pharmacokinetics and tumor uptake in a mouse model. *Cancer Biotherapy Radiopharmaceuticals*. 2018;33(1):8–16. <https://doi.org/10.1089/cbr.2017.2337>.
31. Dai Y-H, Chen P-H, Lee D-J, et al. A meta-analysis and meta-regression of the efficacy, toxicity, and quality of life outcomes following prostate-specific membrane antigen radioligand therapy utilising lutetium-177 and actinium-225 in metastatic prostate cancer. *Eur Urol*. 2024. <https://doi.org/10.1016/j.eururo.2024.09.020>.
32. Rupp NJ, Umbricht CA, Pizzuto DA, et al. First clinicopathologic evidence of a non-psma-related uptake mechanism for 68ga-psma-11 in salivary glands. *J Nucl Med*. 2019;60(9):1270–6. <https://doi.org/10.2967/jnumed.118.222307>.
33. Taïeb D, Foletti J-M, Bardies M, et al. Psma-targeted radionuclide therapy and salivary gland toxicity: why does it matter? *J Nucl Med*. 2018;59(5):747–8. <https://doi.org/10.2967/jnumed.118.207993>.
34. Muniz M, Loprinzi CL, Orme JJ, et al. Salivary toxicity from psma-targeted radiopharmaceuticals: what we have learned and where we are going. *Cancer Treat Rev*. 2024;127. <https://doi.org/10.1016/j.ctrv.2024.102748>.
35. Heynickx N, Segers C, Coolkens A, et al. Characterization of non-specific uptake and retention mechanisms of [177lu]lu-psma-617 in the salivary glands. *Pharmaceuticals*. 2023;16(5). <https://doi.org/10.3390/ph16050692>.
36. Weaver AN, Lakritz S, Mandair D, et al. A molecular guide to systemic therapy in salivary gland carcinoma. *Head Neck*. 2023;45(5):1315–26. <https://doi.org/10.1002/hed.27307>.

Publisher's note Springer Nature remains neutral with regard to jurisdictional claims in published maps and institutional affiliations.

Authors and Affiliations

Huanhuan Liu^{1,2} · Xiaojun Zhang¹ · Jingfeng Zhang^{1,2} · Yue Pan^{1,2} · Hui Wen¹ · Xiaodan Xu¹ · Shina Wu¹ · Yuan Wang¹ · Cong Zhang^{1,2} · Guangyu Ma¹ · Yachao Liu¹ · Ruimin Wang¹ · Jinming Zhang¹ 

✉ Yachao Liu
yachao301@163.com

✉ Ruimin Wang
wrm@yeah.com

✉ Jinming Zhang
zhangjm301@163.com

¹ Department of Nuclear Medicine, The First Medical Centre, Chinese PLA General Hospital, No. 28 Fuxing Road, Haidian District, Beijing 100853, China

² Medical School of Chinese PLA, Beijing 100853, China